29th EPS Conference on Plasma Phys. and Contr. Fusion Montreux, 17-21 June 2002 ECA Vol. **26B**, P-4.100 (2002)

Overview of the QPS Project

J.F. Lyon[1], L.A. Berry[1], S.P. Hirshman[1], B.E. Nelson[1], D.A. Spong[1], D.J. Strickler[1], A.S. Ware[2], D.E. Williamson[1], D.B. Batchelor[1], R.D. Benson[1], A. Brooks[3], M.J. Cole[1], A.J. Deisher[2], P.J. Fogarty[1], R.H. Fowler[1], G.Y. Fu[3], P. Goranson[1], D. Heskett[2], D. Mikkelsen[3], P.K. Mioduszewski[1], D.A. Monticello[3], D.A. Rasmussen[1]

[1]Oak Ridge National Laboratory, P.O. Box 2009, Oak Ridge, TN 37831-8072, U.S.A.
[2]Department of Physics and Astronomy, University of Montana, Missoula, MT, 59812, U.S.A
[3]Princeton Plasma Physics Laboratory, P.O. Box 451, Princeton, NJ 08502, U.S.A

Abstract. QPS is a very-low-aspect-ratio stellarator that is quasi-poloidally-symmetric with $\langle R \rangle = 0.9$ m, $\langle a \rangle = 0.33$ m, $\langle B_{axis} \rangle = 1$ T for a 1-s pulse, and $P_{heating}$ = 1-3 MW. The quasi-poloidal symmetry leads to low neoclassical transport at low aspect ratio. This paper describes the physics properties and the engineering design of the QPS experiment.

I. MAGNETIC CONFIGURATION

A quasi-poloidal stellarator with very low plasma aspect ratio ($\langle R \rangle / \langle a \rangle \sim 2.7$, 1/2-1/4 that of existing stellarators) is a new magnetic confinement approach that could ultimately lead to a high-beta ($\langle \beta \rangle$ = 7-15%) disruption-free compact stellarator reactor. The Quasi-Poloidal Stellarator (QPS) [1] shown in Fig. 1 is being developed to test key features of this approach. The shape of the flux surfaces varies from bean-shaped at the high-field ends to nearly triangular in the middle of the long sections. There is also a helical magnetic axis.

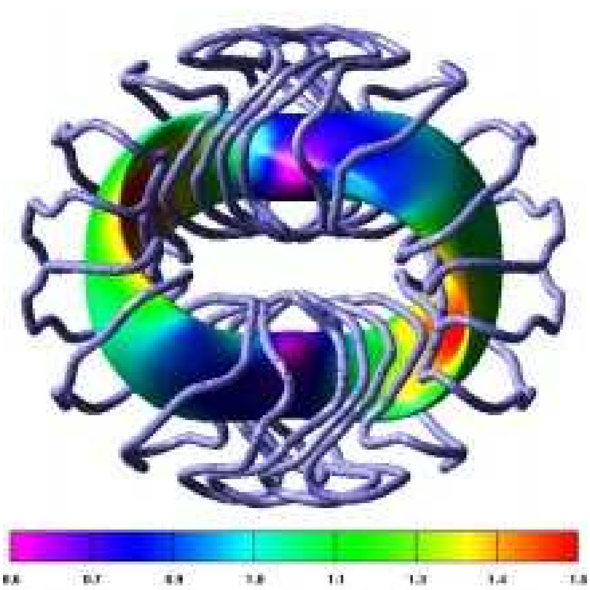

Fig. 1. Top (left) and side (above) views of the QPS plasma and the optimized modular coil geometry used to create it. The colors indicate contours of constant |B in T on the last closed flux surface.

In this approach the dominant components in the magnetic field spectrum are poloidally symmetric in Boozer flux coordinates. Figure 2 shows contours of |B| on two flux surfaces in these coordinates with straight magnetic field lines. The degree of quasi-poloidal symmetry varies with radius *r*. In the plasma core (*r*/<*a*> < 1/2) the magnetic energy in non-poloidally symmetric field components is <10% of that in the poloidally symmetric components; that fraction rises to ~30% at the plasma edge. B and ∇B are more closely aligned than is possible with other forms of symmetry; this reduces banana widths and radial particle drifts out of a flux surface over most of the plasma cross section rather than close alignment of globally averaged drift surfaces and flux surfaces (quasi-omnigenity). However near the edge, quasi-omnigenous features occur that help to reduce neoclassical transport.

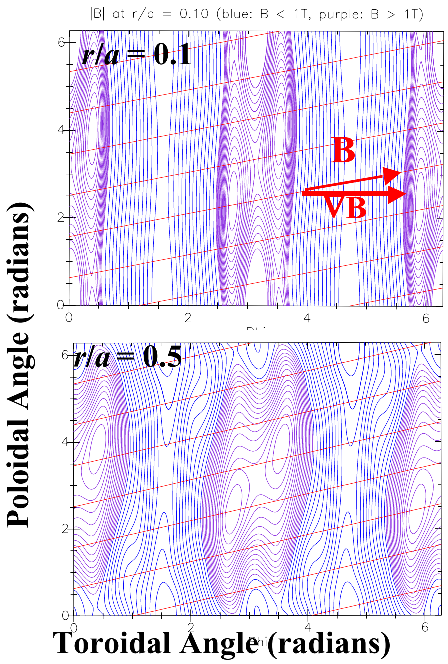

Fig. 2. QPS |B| contours and field lines.

For exact poloidal symmetry, the canonical angular momentum p_θ is conserved and (1) orbit excursions from a flux surface are limited to the gyroradius in the *toroidal* magnetic field ρ_T rather than in the *poloidal* field ρ_p (the banana width) where $\rho_T \ll \rho_p$; (2) there is no flow damping in the poloidal direction; and (3) the bootstrap current is reduced by ι/N where ι is the rotational transform (1/q) and N is the number of toroidal field periods. While exact poloidal symmetry is not possible, quasi-poloidally-symmetric stellarators have these features to a significant extent. In addition: (1) trapped particles are localized in low curvature regions, which should improve stability to dissipative trapped electron modes; and (2) the configuration becomes relatively insensitive to increasing β and the bootstrap current becomes nearly independent of pressure at higher β.

Figure 2 shows that the rotational transform profile can be varied over a large range just by varying the currents in the modular coils by ±25%. Additional control can be obtained by varying the currents in the PF coil sets.

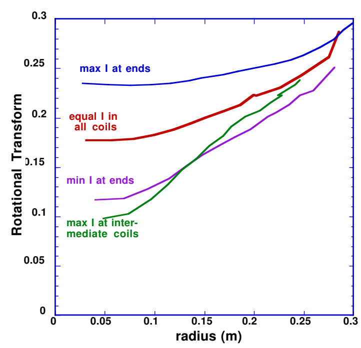

Fig 2 ι variation with modular coil currents.

II. TRANSPORT AND STABILITY

A measure of the reduction in neoclassical transport is shown in Fig. 4. For $E_r = 0$ in the low-collisionality limit, the neoclassical ripple-induced heat diffusivity is proportional to $\varepsilon_{eff}^{3/2}$ where ε_{eff} is the effective ripple in a single helicity 1/ν transport model that gives the same transport as a full 3-D calculation in this limit. QPS has similar transport to that in the W 7-X configuration, but at 1/4 the plasma aspect ratio. Reducing $\varepsilon_{eff}^{3/2}$ further would not be effective since other losses would likely be dominant. The high degree of quasi-poloidal symmetry and the reduced effective field ripple may also reduce the poloidal viscosity, enhancing the naturally occurring E x B poloidal drifts and allowing larger poloidal flow shear damping reduction of anomalous transport.

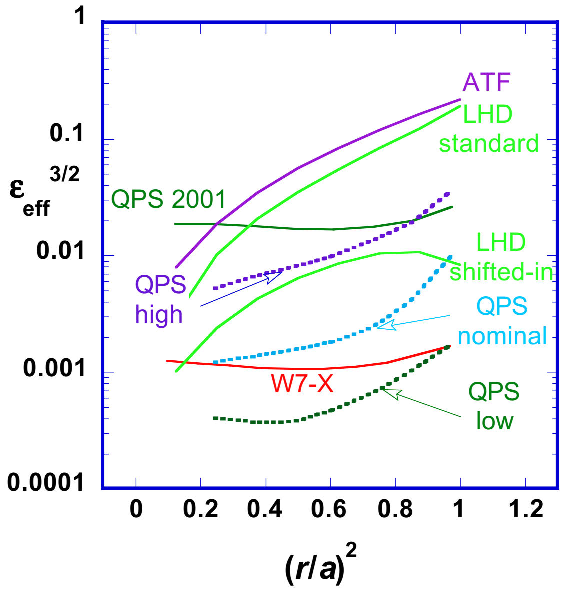

Fig. 4. Coefficient of thermal diffusivity in the 1/ν regime for different stellarators and the variation possible in QPS.

Figure 5 shows that the magnetic surfaces at the two symmetry planes are robust with increasing β; only small magnetic island are seen. Infinite-*n* ballooning modes are stable up to

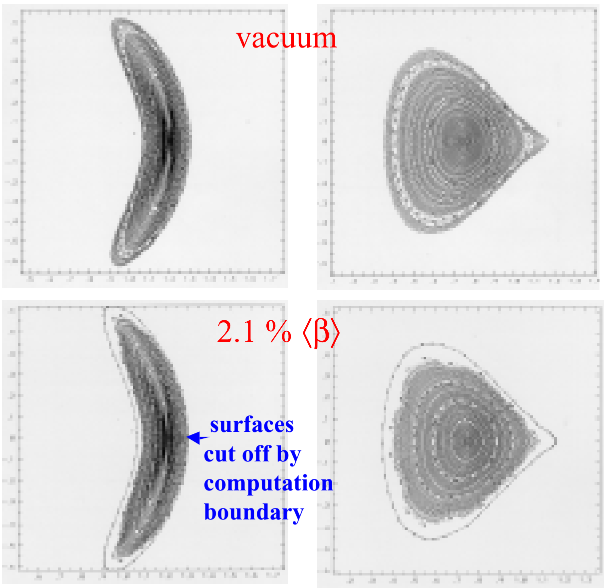

Fig. 5. Magnetic surfaces at the symmetry planes for vacuum and <β> = 2.1%.

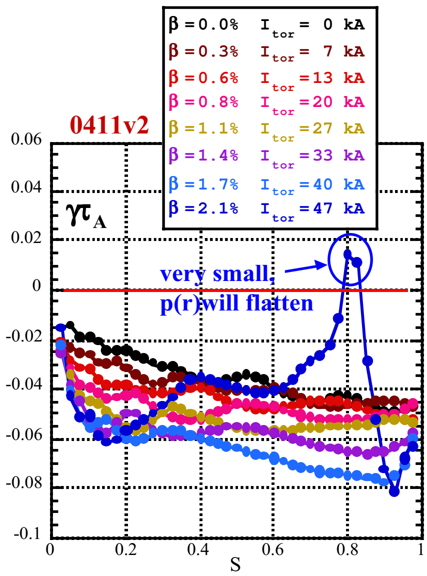

Fig. 6. Normalized ballooning growth rate vs. flux (∝ $\{r/a\}^2$).

<β> > 2%, as shown in Fig. 6. The plasma current required for equilibrium in these free-boundary calculations is consistent with the bootstrap current. Infinite-*n* ballooning modes are unstable for <β> = 2.5-5%, but stable for higher β (second stability region). Kink and vertical modes are stable at <β> ~5% without feedback or conducting walls.

III. ENGINEERING DESIGN

A cutaway view of QPS is shown in Fig. 7 and the main device parameters are listed in Table 1. The main coil set has two field periods with 8 modular coils per period. Due to stellarator symmetry, only four different coil types are needed. The two winding packs that form the coils are separated by a thin stainless steel structural "T" except in the center of the long section where the winding packs follow independent paths (with a wider "T") to improve the configuration properties. The central bore contains the central legs of twelve TF coils. There are three sets of poloidal field coils and a central solenoid for plasma shape and position control and for driving up to 150 kA of plasma current. Twelve 61-cm-diameter ports around the midplane and smaller ports on the top and bottom of the vacuum tank provide access for heating, diagnostics, coil services, and instrumentation feedthroughs. First plasma operation is planned for 2007.

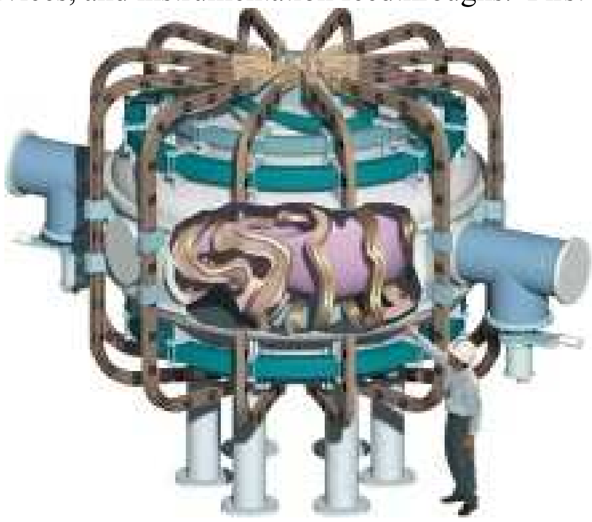

Fig. 7. Cutaway view of QPS.

Table 1. QPS Device Parameters

Ave. major radius <*R*>	0.9 m
Ave. plasma radius <*a*>	0.33 m
Plasma aspect ratio	2.7
Plasma volume V_{plasma}	
Central, edge rotational	2 m^3
transform ι_0, ι_a	0.21, 0.32
Average field on axis	
from modular coils	B_{mod} = 1 T
Auxiliary toroidal field	for1-s pulse
Ohmic current I_{plasma}	± 0.2 T
ECH power	≤ 150 kA
ICRF heating power	0.6-1.2 MW
	1-3 MW

The modular coils have a stainless steel vacuum-tight case since they share the same vacuum as the plasma. Calculations show that field lines leave the plasma predominantly at the top and bottom of the bean-shaped cross sections where recycling neutrals will be confined mechanically by divertor baffles and then be largely reionized by the boundary plasma. Connection lengths in the scrapeoff region are long enough for effective island divertor operation.

Acknowledgments: This work was supported by the U.S. Dept. of Energy under contract DE-AC05-00OR22725 with UT-Battelle, LLC.

[1] J. F. Lyon and the QPS team, "QPS, A Low Aspect Ratio Quasi-Poloidal Concept Exploration Experiment", http://qps.fed.ornl.gov/, April 2001.